



ELSEVIER

doi:10.1016/j.gca.2004.07.033

Potentiometric titrations of *Bacillus subtilis* cells to low pH and a comparison of modeling approaches

JEREMY B. FEIN,^{1,*} JEAN-FRANÇOIS BOILY,² NATHAN YEE,³ DREW GORMAN-LEWIS,¹ and BENJAMIN F. TURNER¹¹University of Notre Dame, Civil Engineering and Geological Sciences, Notre Dame, IN 46556, USA²Swiss Federal Institute of Technology, Institut für Mineralogie und Petrographie CH-8092 Zürich, Switzerland³School of Earth Sciences, University of Leeds, Leeds LS2 9JT, United Kingdom

(Received September 18, 2003; accepted in revised form July 26, 2004)

Abstract—To provide constraints on the speciation of bacterial surface functional groups, we have conducted potentiometric titrations using the gram-positive aerobic species *Bacillus subtilis*, covering the pH range 2.1 to 9.8. Titration experiments were conducted using an auto-titrator assembly, with the bacteria suspended in fixed ionic strength (0.01 to 0.3 M) NaClO₄ solutions. We observed significant adsorption of protons over the entire pH range of this study, including to the lowest pH values examined, indicating that proton saturation of the cell wall did not occur under any of the conditions of the experiments. Ionic strength, over the range studied here, did not have a significant effect on the observed buffering behavior relative to experimental uncertainty. Electrophoretic mobility measurements indicate that the cell wall is negatively charged, even under the lowest pH conditions studied. These experimental results necessitate a definition of the zero proton condition such that the total proton concentration at the pH of suspension is offset to account for the negative bacterial surface charge that tends towards neutrality at pH < 2.

The buffering intensity of the bacterial suspensions reveals a wide spread of apparent pK_a values. This spread was modeled using three significantly different approaches: a Non-Electrostatic Model, a Constant Capacitance Model, and a Langmuir-Freundlich Model. The approaches differ in the manner in which they treat the surface electric field effects, and in whether they treat the proton-active sites as discrete functional groups or as continuous distributions of related sites. Each type of model tested, however, provides an excellent fit to the experimental data, indicating that titration data alone are insufficient for characterizing the molecular-scale reactions that occur on the bacterial surface. Spectroscopic data on the molecular-scale properties of the bacterial surface are required to differentiate between the underlying mechanisms of proton adsorption inherent in these models. The applicability and underlying conceptual foundation of each model is discussed in the context of our current knowledge of the structure of bacterial cell walls. Copyright © 2005 Elsevier Ltd

1. INTRODUCTION

The ability to model proton and metal adsorption onto bacterial cell walls is crucial to understand the effects of bacterial surface complexation on mass transport in geologic systems. A growing number of potentiometric studies of the protonation of bacterial cell walls have been conducted recently (Plette et al., 1995; Fein et al., 1997; Daughney and Fein, 1998; Cox et al., 1999; Haas et al., 2001; Sokolov et al., 2001; Yee and Fein, 2001; Wightman et al., 2001; Martinez et al., 2002; Ngwenya et al., 2003; Yee et al., 2004). However, an almost equally large number of modeling approaches have been used to interpret these potentiometric data. For example, Plette et al. (1995) used a three-site Langmuir-Freundlich model, coupled with the Gibbs-Donnan shell model, to account for their experimental acidimetric titration measurements of *Rhodococcus erythropolis* A177. Fein et al. (1997) conducted potentiometric titrations of *Bacillus subtilis*, and modeled the results with three discrete cell wall functional groups, using a constant capacitance model. Cox et al. (1999), in similar experiments but using a nonelectrostatic (neglecting the effects of the double layer) linear programming method (LPM) modeling approach (Brassard et al., 1990), modeled titration data using five discrete binding sites.

Martinez et al. (2002) interpreted potentiometric titration data for *B. subtilis* and *Escherichia coli* by considering a set of equally spaced ($\Delta pK_a = 0.2$) pK_a values and using the Gibbs-Donnan shell model to account for electrostatic effects, finding evidence for four types of bacterial surface functional groups.

Models of bacterial surface protonation serve two purposes: 1) to elucidate the molecular-scale mechanisms for adsorption reactions that occur between aqueous solutes and the bacterial surface, and 2) to enable quantitative geochemical modeling of mass transport in bacteria-bearing systems. The lack of consensus for a protonation model has hampered efforts to move forward on both of these fronts. Spectroscopic investigations of metal binding on bacterial cell walls provide some constraints to the molecular-scale reactions, but there are only a handful of these studies to date. Furthermore, spectroscopy data can not be used to determine the thermodynamic stability of surface complexes as easily as potentiometric and bulk metal adsorption data.

In this study, we conduct potentiometric titration studies of *B. subtilis* using fixed ionic strength electrolytes that range from 0.01 to 0.3 M. We couple these observations with electrophoretic mobility measurements, conducted as a function of pH. We extend the pH range of our titrations to lower values than most studies have examined in an attempt to attain experimental conditions under which the bacterial cell wall func-

* Author to whom correspondence should be addressed (fein.1@nd.edu).

tional groups are fully protonated. We examine the pH range of ~2 to 10. Bacterial cell walls lose their structural integrity and release significant quantities of cytoplasmic organic molecules at pH values above 10, so titrations can not examine protonation behavior in that pH range. Some structural damage occurs to the cell walls below pH 4 (Borrok et al., 2004b), but it is also clear from bulk adsorption and X-ray absorption spectroscopy results that some cell wall functional groups are proton-active and capable of adsorbing metal cations below this pH (Fowle et al., 2000; Kelly et al., 2002; Boyanov et al., 2003). Therefore, examination of these proton-active sites requires an experimental balance between the needs of probing acidic conditions and those of avoiding acidic structural cell wall damage. The objectives of the study are to determine if the cell wall functional groups are fully protonated under low pH conditions, and to compare the abilities of a range of protonation models to account for the bacterial surface potentiometric titration data, and in so doing, to compare and contrast the strengths and limitations of each modeling approach.

2. MATERIALS AND METHODS

2.1. Growth Conditions

The bacterial species used in this study was the aerobic gram-positive species *Bacillus subtilis*. Bacterial cultures were maintained on trypticase soy agar with 0.5% yeast extract, with new plates inoculated every 1–2 weeks to prevent sporulation. Bacterial cells for experimentation were initially cultured in 3 mL of trypticase soy broth with 0.5% yeast extract for 24 h at 32°C, then transferred to 1 L of broth/yeast extract mixtures and grown for another 24 h with shaking at 32°C. The cells were removed from the nutrient medium by centrifugation, rinsed twice in 0.1 M NaClO₄ (the electrolyte used in the experiments), and soaked in 0.03 mol/L HNO₃ for 30 min to remove contaminant cations from the bacterial surface. The cells that were used in the ionic strength experiments were not acid washed. Cells for all experiments were then rinsed five additional times in NaClO₄ at the concentration to be used in each experiment. The weight of the bacteria used in each experiment was determined as a wet weight after 1 h of centrifugation at 7500 rpm (8000 g). The ratio of this wet weight to the dried weight of the biomass is 5.1:1 (Borrok et al., 2004). Previous work in our laboratory indicates that the wash procedure effectively removes competing cations from the bacterial surfaces without inducing significant sporulation of the cells (Daughney and Fein, 1998).

2.2. Potentiometric Titrations

Potentiometric titrations of concentrated (14.7–29.4 g dry weight/L) biomass suspensions were carried out under a N₂ atmosphere at 298 K. Ionic strength was buffered by suspending the biomass in NaClO₄ electrolyte (0.01, 0.1, or 0.3 M). The titrations were performed with an automated burette assembly, and pH measurements were conducted with a glass combination electrode filled with 4 M KCl. The electrode was standardized using two different approaches: 1) with commercially supplied pH standards, and 2) on a proton concentration scale, [H⁺], such that:

$$E = E_o + 59.156 \log [H^+] + j_{ac} [H^+] \quad (1)$$

where E_o is the standard electromotive force (e.m.f.) of the electrode (V), E is the measured electromagnetic frequency, and j_{ac} is the acidic liquid junction potential coefficient (the alkaline liquid junction potential was not necessary). Rossotti and Rossotti (1961) provide a more complete discussion of this approach. The titrations were carried out by adding a commercially supplied volumetric standard of 1.0005 M HNO₃ and an experimentally restandardized solution of 1.008 M NaOH, standardized against the acid by Gran titrations. Titrant addition was carried out when the stability of the electromagnetic frequency was less than 0.01 mV/s, i.e., the smallest drift allowed by the instrument.

This stability value is sufficient to yield reversible titrations (Daughney and Fein, 1998). The value of j_{ac} and E_o were determined simultaneously from electrolyte solutions titrated from 3.3 to 27 mM [H⁺], where the latter exhibits only a 2.5% deviation from the activity coefficient of singly charged ions in 0.1 M NaClO₄. The determination of j_{ac} extended the reliable working pH range from pH ≈ 2.5, in the case where commercial pH buffers would be used, down to pH ≈ 2.

Before each titration, the biomass suspension was purged of dissolved CO₂ with N₂(g) for 60 min, yielding approximate suspension pH values of 3.7 and 6–7 for the acid-washed and non-acid-washed bacteria, respectively. The suspensions were then titrated acidimetrically to pH ≈ 2 and then alkalimetrically to pH ≈ 10. Above pH 10, significant cell lysis occurs, and may interfere with the buffering measurements. We conducted three types of titrations: 1) blank titrations using 0.1 M NaClO₄ as the background electrolyte, 2) four replicate experiments (hereafter termed “0.1 M bacterial titrations”) using 0.1 M NaClO₄, and 3) six additional experiments to test for an ionic strength dependence to the buffering behavior (hereafter termed “ionic strength titrations”): two titrations each conducted using 0.01, 0.10, and 0.30 M NaClO₄. To minimize and test the possibility of cell wall damage in the ionic strength experiments, the acid wash step in the bacterial preparation was omitted. However, because each suspension was acidified to low pH before the titration experiments, it should be noted that even the bacteria in the ionic strength titrations had to be exposed to low pH conditions during the titrations to probe the protonation behavior that occurs at low pH.

2.3. Electrophoretic Mobility Determination

The electrophoretic mobility of bacterial cells can be used as at least a qualitative indication of the electric charge on a bacterial surface. The electrophoretic mobility of a particle is quantified by measuring the velocity of a particle in an electric field. We measured the electrophoretic mobility of suspensions of *B. subtilis* as a function of pH in 0.1 M NaClO₄ using a Malvern Zetamaster. A known amount of 0.1 M NaOH or HNO₃ was added to a 100 mg/L bacterial suspension to adjust the pH to each desired value. When the pH of the suspension stabilized (± 0.05 pH units), a homogeneous 10-mL aliquot of the suspension was injected into the apparatus. Triplicate electrophoretic mobility measurements were performed. The average analytical uncertainty was ± 0.114 microns/s/V/cm for each condition studied. A single zeta potential transfer standard (silica colloids) with -50 ± 5 mV was used to calibrate the laser-doppler velocimetric device.

3. RESULTS

All data are plotted in terms of moles of deprotonated sites per mass of bacteria (mol/g),

$$[H^+]_{\text{consumed/released}} = (C_a - C_b - [H^+] + [OH^-])/m_b \quad (2)$$

where C_a and C_b are the concentrations of acid and base added at each step of a titration, brackets represent molal species concentrations, and m_b is the bacterial wet weight suspension concentration (g/L). The bacterial suspensions exhibit substantial proton adsorption/desorption over the entire pH range studied. For the 0.1 M bacterial titrations, acidimetric titrations from the pH of immersion at ~3.7 to about pH 2 (data not shown) reveal a total uptake of ~0.09 mM H⁺/g, without any evidence of saturation with respect to proton adsorption. Full protonation of the cell wall functional groups would cause the slope of the suspension titration curve to match that of the blank titration of the 0.1 M NaClO₄ electrolyte under low pH conditions. However, as shown in Figure 1 for one titration example, the bacterial suspension titration curves exhibit steeper slopes than those of the blank electrolyte titrations, indicating that even under the lowest pH conditions of these experiments, full protonation of the cell wall functional groups was not attained.

The bacterial cells display electrophoretic behavior across

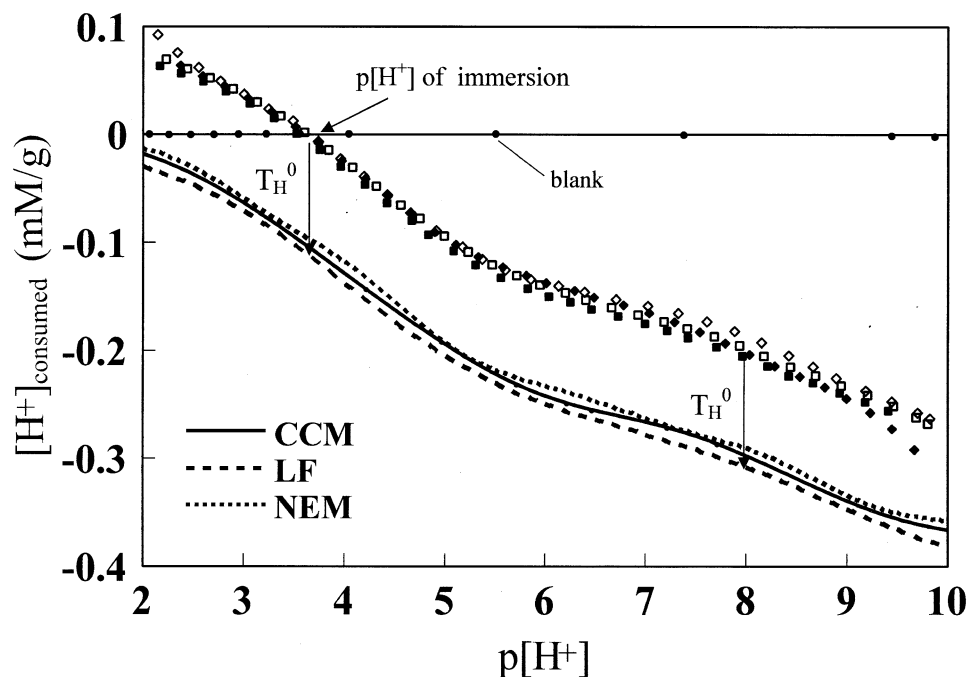


Fig. 1. Potentiometric titration data of 75–150 g/L (wet weight) *Bacillus subtilis* in 0.1 M NaClO₄. The data are calculated with Eqn. 2, i.e., with $[H^+]_{\text{consumed}} = 0$ at the pH of suspension. The model curves are calculated with Eqn. 3, i.e., taking into account T_H^0 . All curves predict negatively charged bacteria surfaces, in accordance with the zeta potential measurements.

the entire pH range of these experiments, with the magnitude of the mobility increasing with increasing pH (Fig. 2). These results indicate that the cell wall is negatively charged between pH 2 to 10, and is most electronegative under alkaline conditions. Although the electronegativity decreases markedly to near-neutral values at $\text{pH} \approx 2$, an electrophoretic mobility value of zero was not observed even at the lowest pH condition studied. Because the surface charge of bacterial cells is established solely by proton dissociation from cell wall ligands, the electrophoretic mobility data provide additional evidence that the surface functional groups are not fully protonated under the

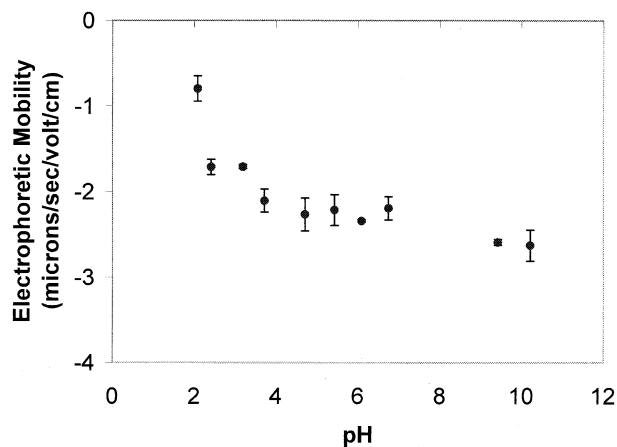


Fig. 2. Electrophoretic mobility measurements conducted using suspensions of *Bacillus subtilis* in 0.1 M NaClO₄ as a function of pH.

experimental conditions. Titrations to pH values < 2 did not yield reproducible results, because of the increasingly demanding precision of the electromagnetic frequency data and the lack of control in the liquid junction potential.

Above pH 3.8, our 0.1 M bacterial titration curves are virtually identical to those observed previously for *B. subtilis* (Fein et al., 1997; Daughney and Fein, 1998; Wightman et al., 2001; Martinez et al., 2002) with a release of 0.26–0.29 mM H^+ /g. The buffering intensity (given by the value $d(\Sigma[R-L^-])/d(\text{pH})$, as calculated from a cubic spline fit) of the suspension (Fig. 3) reveals: 1) nonzero buffering behavior across the pH range of the experiments; 2) a buffering minimum at pH

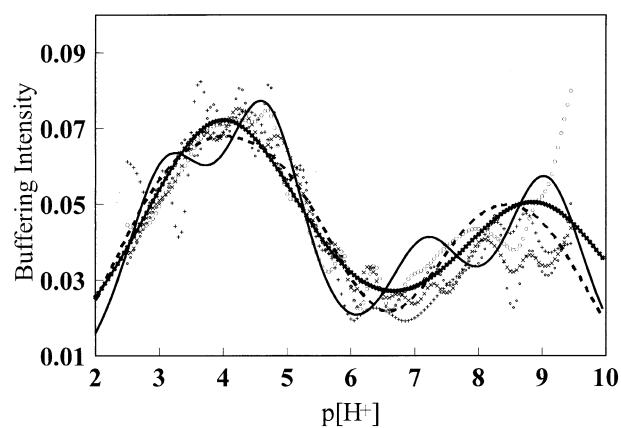


Fig. 3. Experimental (data points) and predicted (smooth curves) buffering intensities (see text).

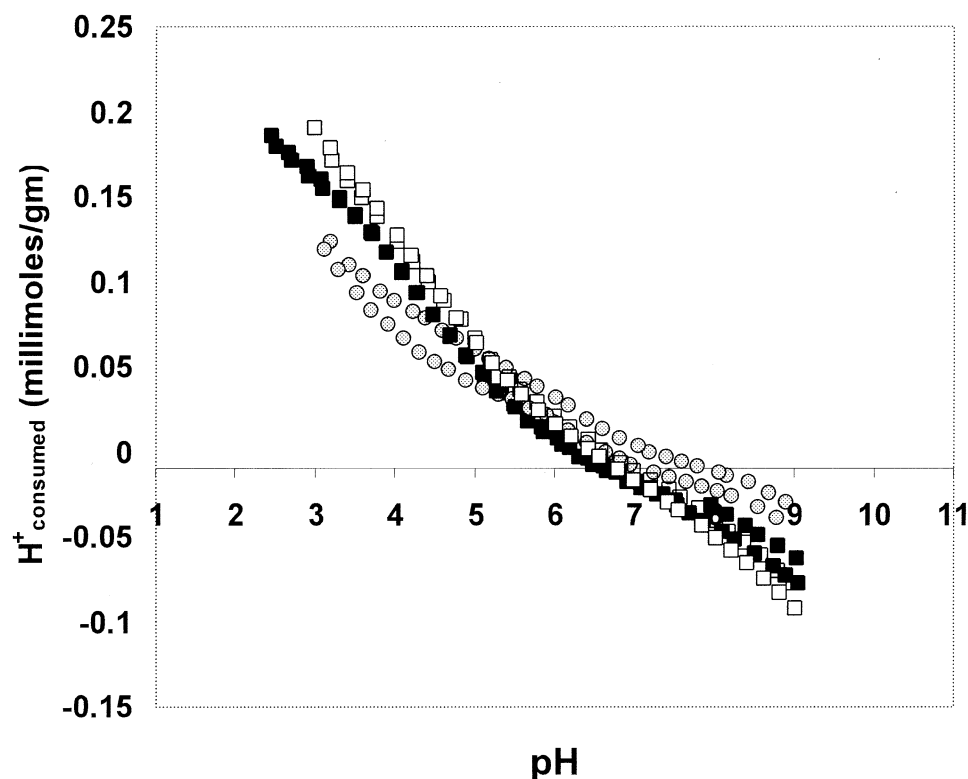


Fig. 4. Potentiometric titration data for suspensions of non-acid-washed *Bacillus subtilis* in 0.01 (circles), 0.1 (open squares), and 0.3 (filled squares) M NaClO₄.

≈ 6–7; 3) one buffering maximum on the acidic site of this minimum; and 4) an increasing buffering intensity with increasing pH at higher pH values. Note that some of the highest and lowest pH datapoints have been eliminated from Figure 3 because of precision difficulties in calculating slopes at the edges of the dataset.

Figure 4 depicts the results from the ionic strength titrations. Although a possible ionic strength effect can be observed over the ionic strength range studied (especially at low pH), the effect is weak compared to the relatively large experimental uncertainties associated with bacterial potentiometric titrations. The uncertainties associated with these experiments are typical of biomass titrations (Fein et al., 1997; Daughney and Fein, 1998; Cox et al., 1999; Yee and Fein, 2001; Martinez et al., 2002), and in any event the effect of ionic strength is small relative to the pH effect on the buffering intensity. We use these data to demonstrate qualitatively the ionic strength dependence of the buffering behavior. Because of the limited pH coverage of these titrations (e.g., to keep ionic strength constant in the 0.01 M electrolyte, acidification to pH values below ~3 is not possible), we do not use the data in the modeling approaches.

4. TOTAL PROTON CONCENTRATION DETERMINATION

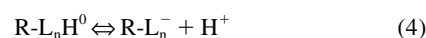
The interpretation of adsorption/desorption studies requires an accurate constraint on the mass balance of the adsorbing species. Potentiometric titration experiments are essentially studies of proton adsorption and desorption, yet because the solvent contains the same element as is reacting with the

surface of interest, it is impossible to apply a traditional mass balance approach. Instead, one must define a zero proton condition for the bacterial cell wall, and account for changes in proton concentrations relative to that condition. Plette et al. (1995) have, for instance, used a common intersection point in titration data at different ionic strengths to identify the zero proton condition of suspensions of *Rhodococcus erythropolis* A177. However, a number of modeling approaches used in previous interpretations of bacterial surface titration data have neglected to explicitly define a zero proton condition, and therefore, have implicitly ignored the problem of defining the initial “total” H (T_H^0) concentration in the experimental systems. The problem of determining the value of T_H^0 is discussed in more detail by Westall et al. (1995).

The mass balance for the total proton concentration in the system can be written as

$$T_H = T_H^0 + (C_a - C_b) \quad (3)$$

where T_H is the total proton concentration of protons in the system at any point during the potentiometric titration, T_H^0 is the initial total concentration of H at the commencement of the titration, and C_a and C_b refer to the concentration of acid and base, respectively, added to the system during the titration. The sink in the proton budget, as pH is varied, is then ascribed to the (de)protonation of bacterial cell wall functional groups, $R-L_nH^0$ according to the following reaction stoichiometry:



This model is consistent with the electrophoretic mobility measurements which suggest that at a low pH value (less than those studied here), the bacterial cell wall becomes uncharged. With increasing pH above this neutral point, the cell wall becomes increasingly negatively charged as deprotonation reactions (e.g., reaction (4)) proceed from left to right.

Clearly, it is crucial to determine T_H accurately because it is the parameter that is used to constrain the total concentration of deprotonated sites ($\sum[R-L_n^-]$) at each point of the titration through the proton mass balance constraint:

$$T_H = [H^+] - [OH^-] - \sum [R-L_n^-] \quad (5)$$

where the summation is taken over all types of functional groups, n .

Unlike bulk metal adsorption experiments, which typically start with an initial metal concentration of zero before the addition of metal to the system, potentiometric titration experiments are conducted in a system awash in hydrogen, both as H_2O molecules and as H^+ ions in solution and adsorbed to surface functional groups. Therefore, to practically establish mass balance constraints on hydrogen, a “zero proton condition” for the bacterial cell wall must be defined at which $T_H^0 = 0$. For mineral surfaces, this condition is defined as the isoelectric-point/point-of-zero-charge of the mineral. For organic ligands, such as those on bacterial surfaces, one can choose either the fully protonated state or the fully deprotonated state. Because the bacteria undergo extensive lysis under high pH conditions, and because the initial bacterial suspension in these experiments is relatively low in pH, we choose the fully protonated bacterial cell wall to represent our zero proton condition.

As noted by Westall et al. (1995), the value of $C_a - C_b$ at each titration point can be determined precisely, but the value of T_H^0 is much more difficult to constrain because it requires some knowledge of the *initial* protonation state of the functional groups in the system of interest. If one makes the erroneous assumption that $T_H = C_a - C_b$ (in effect ignoring the contribution made by T_H^0) at the pH of immersion, then the titration is assumed to begin at the zero proton condition. Moreover, this assumption imposes that:

$$[H^+]_{\text{immersion}} - [OH^-]_{\text{immersion}} = \sum [R-L_n^-] \quad (6)$$

at the pH of immersion. In the case of the bacterial suspensions considered in this study (which have a suspension pH of ~ 3.7), this assumption would require that $\sum[R-L_n^-] = 10^{-3.7}$ M for 100–150 g/L. The data of Figures 1 and 2, however, show that the bacteria can sorb up to 0.09 mM/g protons down to $pH \approx 2$ without fully protonating the cell wall. Potentiometric titrations yield no information on the sign or magnitude of the surface charge, and we assume that the bacterial surface charge tends to zero at pH values < 2 . The possibility that *B. subtilis* develops a positive surface charge arising from amino groups at low pH is also neglected at present in the absence of supporting evidence (e.g., discernable ionic-strength dependent isoelectric points).

5. MODELING APPROACHES

The general expression for the total concentration of deprotonated sites on the bacterial surface can be written

$$\sum [R-L_n^-] = \sum_1^n \frac{[R-L_nH]_{\text{Tot}}}{1 + a_{H^+} \cdot \beta_n} \quad (7)$$

where the expression is summed for each of the n functional groups on the cell wall, $[R-L_nH]_{\text{Tot}}$ is the total molar concentration of the n^{th} functional group, and β_n is its associated acidity constant:

$$\beta_n = \frac{[R-L_n^-]a_{H^+}}{[R-L_nH^0]} \quad (8)$$

where the brackets denote concentration units in moles of sites / L and a represents the activity of the subscripted aqueous species. We refer to β_n values that are referenced to zero ionic strength and zero net surface charge as thermodynamic acidity constants, or “pKa” for the negative logarithm of these values.

Our titration experiments demonstrate that the buffering capacity of the bacterial cell wall extends over a wide pH range. The modeling approaches that we consider account for the broad buffering capacity in one of two ways: either by invoking a limited number of “discrete” sites, each with its own values for site concentration and β_n , or by decreasing the step size between β_n values to create infinitesimal steps in $\delta \beta_n$, and thereby obtaining a continuous distribution of acidity constants about a modal value $\tilde{\beta}_n$.

5.1. Non-Electrostatic Model and Constant Capacitance Model

The Non-Electrostatic Model (NEM) employs Eqns. 7 and 8 to account for the buffering behavior without alteration of the β_n values (James and Parks, 1975). The stoichiometry of reaction 4 constrains the buffering intensity of each functional group to occupy a relatively narrow pH range. For example, when $pH = p\beta_n$, 50% of the sites are protonated; when $pH = p\beta_n + 1$, only 10% of the sites are protonated, with a corresponding decrease in buffering intensity. The buffering intensity peaks shown in Figure 3 are broader than can be accounted for with single functional groups using the NEM. Therefore, when modeling the data with the NEM, additional functional groups must be invoked to account for the broader pH range for the observed buffering intensity.

Alternatively, the broad buffering intensity peak can be accounted for with fewer discrete sites using the Constant Capacitance Model (CCM) (Hohl and Stumm, 1976). In the CCM, the intrinsic discrete acidity constant of a site is shifted, and its pH range of influence broadened, by an electrostatic potential, Ψ , at the so-called bacteria/water interface such that:

$$p\beta_n = p\beta_{n,\text{int}} - F\Psi \cdot (2.303 RT)^{-1} \quad (9)$$

where F is Faraday’s constant and R the molar gas constant. In this approach, the acidity is incrementally decreased by any incremental increase in Ψ that is related to the bacterial charge concentration through a constant capacitance, C :

$$\frac{\sum [R-L_n^-] \cdot F}{m_b} = C \cdot \Psi \quad (10)$$

This formalism assumes a two-dimensional disposition of the bacterial surface functional groups to form a Helmholtz-like

compact layer, clearly a simplification of the bacterial binding sites, which are likely located within the three-dimensional, ~25-nm-thick peptidoglycan layer of the cell wall, and not on a single plane (Beveridge and Murray, 1980; Fortin et al., 1997).

5.2. Langmuir-Freundlich Model

The Langmuir-Freundlich Model (LFM) is a useful alternative to the multisite NEM and the CCM approaches. Instead of using a combination of sites with various discrete values for $p\beta_n$, the LFM approach invokes a continuous distribution of acidity constants about a modal value $\tilde{\beta}_n$. The analytical expression of this idea in the context of a gaussian distribution of β_n is given by the LFM (Koopal et al., 1994):

$$\sum [R - L_n^-] = \sum_1^n \frac{[R - L_n H]_{Tot}}{1 + (a_{H^+} \cdot \beta_n)^{m_n}} \quad (11)$$

where the factor m_n , scaled from 0 to 1, affects the width of the distribution of the n^{th} proton-active site. The n^{th} site with a modal value $\tilde{\beta}_n$ may then be said to exhibit gaussian distribution of β_n , likely resulting from both chemical heterogeneity and electrostatic effects. The contributions of electrostatics (i.e., those that are affected by ionic strength such as diffuse layers or Gibbs-Donnan potentials) may also be separated through the Master Curve approach (Plette et al., 1995). However, our measurements of the ionic strength dependence of bacterial cell wall buffering capacities, along with similar measurements by previous studies, suggest that the ionic strength effect is extremely weak compared to the pH effect. For example, Plette et al. (1995) recorded a difference in bacterial surface charge at pH 7 of ~0.015 meq/g between bacterial suspensions in 0.01 and 1.00 M NaNO₃. This difference is over an order of magnitude smaller than the ~0.70 meq/g difference in relative charge for the bacterial cell wall between pH 3 and 10. van der Wal et al. (1997) observed a more significant ionic strength effect on cell wall protonation behavior, but they used isolated cell wall fragments in their experiments, which may behave differently than whole cells. Potentiometric titrations of *B. subtilis* and *E. coli* cells, conducted by Martinez et al. (2002), are virtually identical over the ionic strength range of 0.01 to 0.50 M KNO₃, and those by Yee et al. (2004) for *B. subtilis* are virtually identical over the ionic strength range of 0.001 to 0.1 M KNO₃. These observations, coupled with the weak ionic strength dependence observed in this study (Fig. 4), lead us to suggest that reasonable approximations of bacterial cell wall buffering capacities can be attained by neglecting ionic strength effects on the buffering behavior.

5.3. Modeling Tools

For each of the modeling approaches, we use two optimization procedures: 1) FITEQL (Westall, 1982) for optimization of the data compiled in terms of pH; and 2) Matlab for optimization of the data compiled in terms of $p[H^+]$. This range of modeling tools is not meant to be all-inclusive, but rather to represent some of the most common tools used in these types of calculations. Westall et al. (1995) presented a method for using FITEQL to solve for T_{II}^0 from a potentiometric titration of a

leonardite humic acid. We use this approach to simultaneously solve for T_{II}^0 , the β_n values, and the site concentrations in each model while determining the minimum number of functional group types that are required to fit the data. For each type of model, we sequentially attempt to fit data from one of the four 0.1 M bacterial titrations with increasing numbers of types of sites until we obtain an adequate fit to the experimental data. The value of the variance parameter $V(Y)$ from FITEQL's output is used as the criterion to distinguish which model best fits the experimental data:

$$V(Y) = \frac{\sum \left(\frac{Y_{\text{calc}} - Y_{\text{exp}}}{S_{\text{exp}}} \right)^2}{n_p n_{II} - n_u} \quad (12)$$

where Y_{calc} and Y_{exp} are the calculated and experimental data, S_{exp} is the error associated with the experimental data, n_p is the number of data points, n_{II} is the number of group II components (components for which total and free concentrations are known), and n_u is the number of adjustable parameters.

For the CCM calculations, we systematically vary the assumed capacitance value, C , to determine the best-fitting value for each dataset. For the LFM optimization calculations, values of m_1 and m_2 are assumed to be equal, primarily because of a lack of independent constraints on the relative distribution of deprotonation behaviors of the two sites. When FITEQL is used for the LFM calculations, we edit the NEM input file, modifying the lines for the mass action (Matrix A) and mass balance (Matrix B) equations. The optimization is carried out using the jacobian that is defined by the computer code, optimizing $\log K$ for the deprotonation reaction(s) for different values of m_n entered as a stoichiometric coefficient in Matrix A. The correct mass balance for protons is ensured in Matrix B and the value of $\log \beta_n$ is given as $\log \beta_n = m_n^{-1} \cdot \log(K)$. Similar to the CCM calculations, we systematically vary the assumed value of m_n to determine the best-fitting value for each dataset.

In addition to using the above range of models, we also demonstrate an approach that extends the usable data to lower pH values. In the traditional approach, we use FITEQL to model C_a-C_b as a function of pH, where pH is directly determined experimentally using commercial pH buffers. In this approach, we use the Davies equation within FITEQL to account for activity coefficients. In the second approach, for each type of model (NEM, CCM, and LFM), the same set of equations are solved in Matlab, modeling C_a-C_b as a function of $p[H^+]$ values as determined by calibrating the pH electrode with Eqn. 1. The extracted j_{ac} value extends the usable data to $p[H^+]$ 2, compared to 2.5 with commercial pH buffers. In Matlab, the values are co-optimized simultaneously using a Levenberg-Marquardt approach by fitting the data in the least square sense and using finite differences to approximate the jacobian.

6. MODELING RESULTS

All modeling results are compiled in Tables 1 and 2, and the model fits for a representative titration are depicted in Figure 1. We used each approach to solve for model parameters for each of the 0.1 M bacterial titrations separately, and we compile the average parameter values in Table 2. As Table 1 indicates for

Table 1. Non-Electrostatic Model fits of one titration.

# of Sites	Log K values	[Site] ^a	V(Y)
1	4.6	169	303.1
2	4.2, 8.0	144, 90	53.4
3	3.5, 5.1, 8.6	89, 90, 84	4.7
4	3.3, 4.7, 6.8, 8.9	75, 96, 31, 75	1.2
5	Does not converge		

^a Site concentrations in $\mu\text{mol/g}$.

the NEM fits to one of the titrations, a four-site model yields an excellent fit to the experimental data. The V(Y) values, from nonelectrostatic models with different numbers of discrete sites, decrease by approximately an order of magnitude with each additional site considered, until the five-site models, none of which converge. This lack of convergence of the model indicates that the system was under-constrained and that the data do not support a model with five discrete functional group types. In all cases for the nonelectrostatic models, a four-site model matches the pH dependence of the buffering capacity significantly better than does a three-site model. This increased fit is reflected in the significantly improved V(Y) value, and its proximity to a value of 1.0, as shown in Table 2. Furthermore, the 0.1 M ionic strength titration data obtained using non-acid-washed bacteria yield identical results (not compiled separately) to the 0.1 M bacterial titrations, which used acid-washed bacteria. This demonstrates that either the acid wash exerts no effect on the titrations, or that the initial acidification step in the titration (which is an unavoidable step if the low pH proton adsorption behavior is to be investigated) is equivalent to an acid wash.

Although the four-site NEM provides an excellent fit to the experimental data, the fit is not a unique one. A range of constant capacitance models can provide equally good fits. For example, a two-site CCM fit to the experimental data is shown in Figure 1 and is compared to the fit provided by the nonelectrostatic model. Clearly, both models yield excellent fits to the

experimental data, demonstrating that there is no unique model that can account for the titration data. A one-site CCM, regardless of the capacitance value used, provides a significantly worse fit to the experimental data than do models with more sites. However, two-, three-, and four-site CCMs yield equally good fits to the data.

The lower the number of sites considered in the CCMs, the lower is the best-fitting capacitance value. For example, the best-fitting capacitance value for the two-site model is 1.2, whereas that for a four-site model is 8.0 F/g. A value of 8.0 F/g implies an extremely small electric field effect and, in essence, a model with such a high capacitance value is a nonelectrostatic model as the thickness of a compact layer is inversely proportional to the capacitance (Hunter, 1981). Our four-site, high capacitance value model is equivalent to that created by Fein et al. (1997). Lower capacitance values tend to widen the calculated pH range over which a functional group deprotonates, similarly widening the calculated buffering capacity of the functional group. Therefore, models with lower capacitance values can account for an observed buffering capacity across the pH range with fewer sites than models with higher C values. The electric field correction also acts to shift the intrinsic acidity constant value relative to the empirically determined pH range of deprotonation, as may be appreciated by Eqns. 9 and 10.

As Figure 1 illustrates, the LFM approach can also yield an equally good fit to the titration data. The LFM parameters, shown in Table 2, predict a zero surface charge at $\text{pH} \approx 1.5$. The acidity constant and site concentration values for the most acidic site are then tightly constrained in the LFM by this zero proton condition and by the buffering minimum at $\text{pH} \approx 6-7$. However, the site concentration and acidity constant value for the second site are not as well constrained, likely due to: 1) the restricted pH range of the experimental data considered, limited by the onset of lysis in alkaline conditions and not sufficient to fully constrain the alkaline buffering maximum; 2) the continuously increasing buffering intensity such that $\text{p}\beta_2 \gg 8$; and 3) the imposed value of $m_1 = m_2$.

In general, the models based on pH measurements yield

Table 2. Proposed models.

	LFM		2-site CCM		NEM	
	Matlab ^b	FITEQL ^c	Matlab	FITEQL	Matlab	FITEQL
[R-L ₁] ^a	258 ± 42	233 ± 38	250 ± 35	191 ± 27	95 ± 19	81 ± 16
pβ ₁	4.04 ± 0.12	4.16 ± 0.12	3.16 ± 0.13	3.32 ± 0.13	3.1 ± 0.2	3.3 ± 0.2
[R-L ₂] ^a	139 ± 59	137 ± 58	113 ± 34	92 ± 28	125 ± 40	112 ± 36
pβ ₂	8.74 ± 0.42	9.49 ± 0.42	6.12 ± 0.16	6.46 ± 0.16	4.6 ± 0.1	4.8 ± 0.1
[R-L ₃] ^a					48 ± 14	44 ± 13
pβ ₃					6.8 ± 0.3	6.8 ± 0.3
[R-L ₄] ^a					82 ± 23	74 ± 21
pβ ₄					8.7 ± 0.2	9.1 ± 0.2
T _H ⁰ ^a	-99 ± 21	-135 ± 29	-90 ± 17	-124 ± 23	-82 ± 18	-116 ± 25
m	0.49	.46				
C			2.2 F/m ²	1.2 F/m ²		

LFM = Langmuir-Freundlich Model; CCM = Constant Capacitance Model; NEM = Non-Electrostatic Model.

All values are the average values obtained from the four separate 0.1 M bacterial titrations. Reported uncertainties are 1σ errors.

^a Concentrations in $\mu\text{mol/g}$.

^b Matlab calculations conducted using $\text{p}[\text{H}^+]$ in the range 2–10.

^c FITEQL calculations conducted using pH in the range 2.5–10.

similar results to those based on $p[H^+]$ values (Table 2). Because of potential errors introduced due to difficulties associated with activity coefficient calculations and liquid junction potential, it is likely that the models that used $p[H^+]$ values yield more accurate characterization of model parameters than do those using pH values, especially for the most acid functional groups. Regardless of which model is used, the T_H^0 values and the average $p\beta_n$ value for the low $p\beta_n$ site demonstrate that significant deprotonation of the low $p\beta_n$ functional groups was evident even under the lowest pH conditions studied here at the start of each titration. Clearly, the concentration of deprotonated sites is not negligible under the initial experimental conditions, emphasizing the fact that ignoring this effect in determining the T_H values would lead to erroneous calculated thermodynamic parameters. In fact, it is possible that titration to lower pH conditions than were studied here could reveal the presence of even lower $p\beta_n$ sites, although titration to lower pH values would also likely cause more damage to the cell walls as a result of exposure to such acidic solutions (Borrok et al., 2004b).

7. DISCUSSION

Although a number of studies report results from potentiometric titrations of bacterial suspensions, this study is the first to compare the ability of different modeling approaches to account for the same set of titration data. The models that we examined differ substantially in their mathematical approaches; they differ in whether they treat functional groups as discrete sites with relatively large, finite differences in pKa values or as a continuum of sites with infinitesimal differences in pKa values; and they differ in their approaches to quantifying the electrostatic effects of the bacterial surface electric field. Despite these large differences between the models, each model yields an excellent fit to the experimental data. Although the models differ in how they distribute functional groups and in the site concentrations of those functional groups, the calculated total site concentrations are similar, as are the calculated T_H^0 values.

This study underscores the strengths and limitations of using potentiometric titration data to elucidate molecular-scale mechanisms responsible for bacterial surface chemistry. Potentiometric titration data unequivocally demonstrate the pH range in which bacterial surfaces can adsorb and desorb protons from solution, and by extension, the pH range in which bacterial surfaces are likely to interact with aqueous ions through adsorption reactions with these proton-active functional groups. The titration data also quantify the buffering capacity of the cell wall functional groups and in so doing place rigorous constraints on the density of proton-active sites.

As our analysis of the data demonstrates, potentiometric titration data do not provide an unequivocal mechanistic understanding of the proton-active sites within the bacterial cell wall, nor do they unequivocally quantify the charging behavior of the bacterial surface. The models that we use to account for the observed buffering behavior clearly show that a range of molecular-scale interpretations is possible, and there is certainly a much wider range of possible models for the buffering behavior than was demonstrated here. Westall and Hohl (1980) conducted a similar analysis, comparing the ability of five

different electrostatic models of a mineral oxide–solution interface to account for observed pH buffering behavior. Westall and Hohl (1980) concluded that the five models that they considered could provide equivalently good fits to the experimental titration data, and that the experimental data from potentiometric titrations alone are insufficient to provide insight into the physical nature of the interface. Our results support a similar conclusion for bacterial surfaces.

Our data do provide some constraints on the nature of the bacterial cell wall proton-active sites. Figure 3 demonstrates that, in the pH range of this study, the bacteria exhibit two maxima in buffering intensity, defined as the derivative of the titration data shown in Figure 1. In addition, the data unequivocally show that the buffering capacity of *B. subtilis* cells extends to pH conditions as low as at least pH 2. As this study indicates, there are a number of ways to account for the buffering maxima: using models that consider the superposition of relatively high numbers of discrete functional groups, using models that account for the electrostatic effects on a relatively small number of functional groups, or using models that invoke a continuous distribution of functional groups with acidity constants distributed about two mean values.

Spectroscopic data on the mechanisms of metal adsorption onto bacterial surfaces confirm the low pH reactivity of the cell wall, and the available data suggest that more than two types of proton-active sites are responsible for the cell wall reactivity over the pH range of interest. Extended X-ray absorption fine structure (EXAFS) spectroscopy experiments document the existence of metal binding sites that are active below pH 2, and they indicate that this low pH metal binding is predominantly onto phosphoryl functional groups. Kelly et al. (2002) and Boyanov et al. (2003) demonstrate that binding of uranyl and Cd, respectively, onto *B. subtilis* is due primarily to phosphoryl binding below pH values of ~ 4 , with carboxyl binding increasing in importance above pH 4. Furthermore, Boyanov et al. (2003) find evidence for a third type of functional group that becomes active at approximately pH 7. The presence of this third type of site is well-constrained by the EXAFS data of Boyanov et al. (2003), but the chemical composition of the site is not. Clearly, spectroscopy plays a vital role in helping to differentiate between models for proton adsorption onto bacterial surfaces and in determining the molecular-scale mechanisms which serve as a foundation for each model.

Whether the bacterial cell wall site responsible for proton uptake and release under low pH conditions is a discrete site or is part of a continuum of related sites, the cellular function of the site for a bacterial species such as *Bacillus subtilis* that thrives best under circumneutral pH conditions is puzzling. A number of explanations are possible to account for the existence of buffering capacity under low pH conditions. Perhaps the site(s) responsible for the buffering enables the bacteria to adsorb inorganic nutrients under occasional low pH episodes; perhaps the site is a structural remnant due to an evolutionary history for this species in acidic environments such as hot springs; or perhaps the site serves as a buffering acid defense mechanism to protect the cell from occasional acid shock events. Clearly, our data do not elucidate the function of this functional group, but our results do show that this site must be considered when modeling the effects of bacterial adsorption

on proton and metal budgets in bacteria-bearing aqueous systems.

8. CONCLUSIONS

Unlike simple organic acids, bacteria exhibit buffering behavior over a large pH range. The buffering intensity of the bacterial cell walls is characterized by two broad peaks of maximum buffering intensity: one at pH 4–5 and one above pH 8.5. This study demonstrates that the observed buffering behavior and intensity can be modeled either with a relatively large number (four) of discrete proton-active sites that are unaffected, or only minimally affected, by surface electric field effects, or with fewer sites that are proton-active over a wider pH range than the discrete sites in the “nonelectrostatic” models. The wider pH range of influence can be caused either by the effects of a bacterial surface electric field, or it may be the result of “site” heterogeneity, or it may result from a combination of the two effects.

Our data indicate that functional groups on the bacterial surface are proton-active over the entire pH range studied here, including down to pH values of as low as 2. This study compares the abilities of dramatically different types of surface protonation models to account for the observed buffering capacity of the bacteria. Each of the models, each with different underlying proton adsorption mechanisms, yields an excellent fit to the data, underscoring the fact that while potentiometric titrations are extremely useful in constraining the thermodynamic properties of bacterial surface functional groups, the titration data alone do not provide structural information about the cell wall. The models presented here represent a relatively small percentage of the wider range of possible models of bacterial surface protonation behavior. It is likely that we could obtain equally good fits to the experimental data using a number of other types of models. This study unequivocally demonstrates that surface charge properties and protonation mechanisms can not be uniquely determined from potentiometric titrations alone. Potentiometric titration data must be considered in conjunction with additional evidence such as spectroscopic data to fully characterize the bacterial surface and to constrain the molecular-scale mechanisms of proton attachment. In the absence of such additional data, the choice of model for the protonation of bacterial surfaces should be made according to the needs of each application.

Acknowledgments—Acknowledgment is made to the Donors of the Petroleum Research Fund, administered by the American Chemical Society, for partial support of this research. Additional support was provided by National Science Foundation grant EAR99-05704 and an Environmental Molecular Science Institute grant (EAR02-21966). N.Y. was also funded by the Leverhulme Trust grant number F-00122/F. We would like to thank Peter Wightman for helpful discussions regarding our interpretation of the potentiometric titration data, and David Ams for preparation of some of the bacteria used in these experiments. Three journal reviews, and the comments made by Associate Editor Michael Machesky, were particularly helpful in improving the presentation of the work.

Associate editor: M. L. Machesky

REFERENCES

- Beveridge T. J. and Murray R. G. E. (1980) Sites of metal deposition in the cell wall of *Bacillus subtilis*. *J. Bacteriol.* **141**, 876–887.

- Borrok D, Fein J. B., and Kulpa C. F. (2004a) Proton and Cd sorption onto natural bacterial consortia: Testing universal adsorption behavior. *Geochim. Cosmochim. Acta* **68**, 3231–3238.
- Borrok D, Fein J. B., Tischler M., O'Loughlin E., Meyer H., Liss M., and Kemner K. (2004b) The effect of acidic solutions and growth conditions on the adsorptive properties of bacterial surfaces. *Chem. Geol.* **209**, 107–119.
- Boyanov M. I., Kelly S. D., Kemner K. M., Bunker B. A., Fein J. B., and Fowle D. A. (2003) Adsorption of cadmium to *Bacillus subtilis* bacterial cell walls: A pH-dependent X-ray absorption fine structure spectroscopy study. *Geochim. Cosmochim. Acta* **67**, 3299–3311.
- Brassard P., Kramer J. R., and Collins P. V. (1990) Binding site analysis using linear programming. *Environ. Sci. Technol.* **24**, 195–201.
- Cox J. S., Smith D. S., Warren L. A., and Ferris F. G. (1999) Characterizing heterogeneous bacterial surface functional groups using discrete affinity spectra for proton binding. *Environ. Sci. Technol.* **33**, 4514–4521.
- Daughney C. J. and Fein J. B. (1998) The effect of ionic strength on the adsorption of H^+ , Cd^{2+} , Pb^{2+} and Cu^{2+} by *Bacillus subtilis* and *Bacillus licheniformis*: A surface complexation model. *J. Colloid Interface Sci.* **198**, 53–77.
- Fein J. B., Daughney C. J., Yee N., and Davis T. (1997) A chemical equilibrium model for metal adsorption onto bacterial surfaces. *Geochim. Cosmochim. Acta* **61**, 3319–3328.
- Fortin D, Ferris F. G., and Beveridge T. J. (1997) Surface-mediated mineral development by bacteria. In *Geomicrobiology: Interactions Between Microbes and Minerals* (eds. J. F. Banfield and K. H. Nealson) *Rev. Mineral.* **35**, 161–180. Mineral. Soc. Amer., Washington, DC.
- Fowle D. A., Fein J. B., and Martin A. M. (2000) Experimental study of uranyl adsorption onto *Bacillus subtilis*. *Environ. Sci. Technol.* **34**, 3737–3741.
- Haas J. R., Dichirstina T. J., and Wade R., Jr. (2001) Thermodynamics of U(VI) sorption onto *Shewanella putrefaciens*. *Chem. Geol.* **180**, 33–54.
- Hohl H. and Stumm W. (1976) Interaction of Pb^{2+} with hydrous $\alpha-Al_2O_3$. *J. Colloid Interface Sci.* **55**, 281–288.
- Hunter R. J. (1981) *Zeta Potential in Colloid Science*. Academic Press, London.
- James R. O. and Parks G. A. (1975) Adsorption of zinc(II) at the cinnabar (HgS)/H₂O interface. *Am. Inst. Chem. Eng. Symp. Ser. (150)* **71**, 157–164.
- Kelly S. D., Boyanov M. I., Fein J. B., Fowle D. A., Yee N., and Kemner K. M. (2002) X-ray absorption fine structure determination of pH-dependent U-bacterial cell wall interactions. *Geochim. Cosmochim. Acta* **66**, 3855–3871.
- Koopal L. K., van Riemsdijk W. H., DeWit J. C. M., and Benedetti M. F. (1994) Analytical isotherm equations for multicomponent adsorption to heterogeneous surfaces. *J. Colloid Interface Sci.* **166**, 51–60.
- Martinez R. E., Smith D. S., Kulczycki E., and Ferris F. G. (2002) Determination of intrinsic bacterial surface acidity constants using a Donnan shell model and a continuous pK_a distribution method. *J. Colloid Interface Sci.* **253**, 130–139.
- Ngwenya B. T., Sutherland I. W., and Kennedy L. (2003) Comparison of the acid-base behaviour and metal adsorption characteristics of a gram-negative bacterium with other strains. *Appl. Geochem.* **18**, 527–538.
- Plette A. C. C., van Riemsdijk W. H., Benedetti M. F., and Van der Wal A. (1995) pH dependent charging behavior of isolated cell walls of a gram-positive soil bacterium. *J. Colloid. Interface Sci.* **173**, 354–363.
- Rossotti F. J. C. and Rossotti H. (1961) *The Determination of Stability Constants*. McGraw-Hill, New York.
- Sokolov I., Smith D. S., Henderson G. S., Gorby Y. A., and Ferris F. G. (2001) Cell surface electrochemical heterogeneity of the Fe(III)-reducing bacteria *Shewanella putrefaciens*. *Environ. Sci. Technol.* **35**, 341–347.
- van der Wal A., Norde W., Zehnder A. J. B., and Lyklema J. (1997)

- Determination of the total charge in the cell walls of Gram-positive bacteria. *Colloids and Surfaces B: Biointerfaces* **9**, 81–100.
- Westall J. C. (1982) *FITEQL, A computer program for determination of chemical equilibrium constants from experimental data*. Version 2.0. Report 82-02, Dept. Chem., Oregon St. Univ., Corvallis, OR, USA.
- Westall J. and Hohl H. (1980) Comparison of electrostatic models for the oxide–solution interface. *Adv. Colloid Interface Sci.* **12**, 265–294.
- Westall J. C., Jones J. D., Turner G. D., and Zachara J. M. (1995) Models for association of metal ions with heterogeneous environmental sorbents. 1. Complexation of Co(II) by leonardite humic acid as a function of pH and NaClO₄ concentration. *Environ. Sci. Technol.* **29**, 951–959.
- Wightman P. G., Fein J. B., Wesolowski D. J., Phelps T. J., Benezeth P., and Palmer D. A. (2001) Temperature dependence of surface protonation reactions occurring at the bacteria–water interface. *Geochim. Cosmochim. Acta* **65**, 3657–3669.
- Yee N. and Fein J. B. (2001) Cd adsorption onto bacterial surfaces: A universal adsorption edge? *Geochim. Cosmochim. Acta* **65**, 2037–2042.
- Yee N, Fowle D. A., and Ferris F. G. (2004) A Donnan potential model for metal adsorption onto *Bacillus subtilis*. *Geochim. Cosmochim. Acta* **68**, 3657–3664.